Andreev Bound States in High Temperature Superconductors

L. Alff, S. Kleefisch, U. Schoop, M. Zittartz, T. Kemen, T. Bauch, A. Marx, and R. Gross

II. Physikalisches Institut, Universität zu Köln, Zülpicherstr. 77, D - 50937 Köln, Germany

Abstract. Andreev bound states at the surface of superconductors are expected for any pair potential showing a sign change in different k-directions with their spectral weight depending on the relative orientation of the surface and the pair potential. We report on the observation of Andreev bound states in high temperature superconductors (HTS) employing tunneling spectroscopy on bicrystal grain boundary Josephson junctions (GBJs). The tunneling spectra were studied as a function of temperature and applied magnetic field. The tunneling spectra of GBJ formed by $YBa_2Cu_3O_{7-\delta}$ (YBCO), $Bi_2Sr_2CaCu_2O_{8+\delta}$ (BSCCO), and $La_{1.85}Sr_{0.15}CuO_4$ (LSCO) show a pronounced zero bias conductance peak that can be interpreted in terms of Andreev bound states at zero energy that are expected at the surface of HTS having a d-wave symmetry of the order parameter. In contrast, for the most likely s-wave HTS $Nd_{1.85}Ce_{0.15}CuO_{4-y}$ (NCCO) no zero bias conductance peak was observed. Applying a magnetic field results in a shift of spectral weight from zero to finite energy. This shift is found to depend nonlinearly on the applied magnetic field. Further consequences of the Andreev bound states are discussed and experimental evidence for anomalous Meissner currents is presented.

Dedicated to J. Zittartz on the occasion of his 60th birthday

PACS. 74.25.Fy Transport properties – 74.50.+r Proximity effects, weak links, tunneling phenomena, and Josephson effects – 74.72.-h High-T sub c compounds – 74.76.Bz High-T sub c films

1 Introduction

Recent experimental and theoretical work on the symmetry of the order parameter in the high temperature superconductors (HTS) has led to the conclusion that for the majority of the cuprate superconductors the symmetry of the order parameter is dominated by a $d_{x^2-y^2}$-wave component [1,2]. This is in clear contrast to the metallic low-temperature superconductors for which the order parameter is dominated by an isotropic s-wave component. The s-wave order parameter usually has the full symmetry of the point group of the underlying crystal structure and, hence, at the transition to the superconducting state only the global gauge symmetry is broken. Such pairing symmetry is denoted conventional. In contrast, the d-wave order parameter of the cuprate superconductors may not have the full symmetry of the point group of the crystal structure and, hence, beyond the global gauge symmetry a further symmetry is broken at the transition to the superconducting state. Such pairing symmetry then is denoted unconventional. An important characteristic of the $d_{x^2-y^2}$-symmetry of the order parameter prevailing in most HTS is a sign change of the pair potential in orthogonal k-directions what is equivalent to a π-phase shift of the wave function. Usually the positive sign is taken along the a-axis of the unit cell and the negative sign along the b-axis. Furthermore, there are nodes of the pair potential in the [110] directions, where it changes sign. That is, the

quasiparticles with corresponding k-vector actually feel a vanishing pair potential what allows for low energy quasiparticle excitations. This is in contrast to a s-wave symmetry, where a finite gap on the whole Fermi surface does not allow for quasiparticle excitations of arbitrarily small energy. We note that the actual order parameter present in hole doped HTS likely is formed by a mixture of a dominating $d_{x^2-y^2}$-component and other components such as an s- or d_{xy}-component. Furthermore, there is evidence that the order parameter of the the electron doped HTS $Nd_{1.85}Ce_{0.15}CuO_{4-y}$ (NCCO) has a dominating s-wave component and no sign change in different k-directions.

There have been numerous experiments devoted to the determination of the symmetry of the order parameter in the oxide superconductors. These experiments can be devided into those probing the amplitude by studying the quasiparticle excitation spectrum and those probing the phase of the order parameter in interferometer experiments employing multiply connected superconductors. Certainly, the key experiments have been the phase sensitive experiments designed by Tsuei and Kirtley which employ HTS thin film tricrystals [3,4]. In these experiments a scanning SQUID-system has been used to show that there are half-integer flux quanta in superconducting rings formed by three differently oriented HTS grains connected by grain boundary Josephson junctions. In this article we present a new class of phase sensitive experiments making use of the formation of Andreev bound states at surfaces

of HTS oriented parallel to the c-axis. An important consequence of an order parameter showing a sign change (or π phase shift) in different k-directions, is the formation of Andreev bound states at zero energy confined to the surface. Andreev bound states have been discussed first in the context of tunneling into unconventional superconductors by Buchholtz and Zwicknagel [5]. Later on, the formation of Andreev bound states or midgap surface states having zero energy with respect to the Fermi energy and sizable areal density as a consequence of a $d_{x^2-y^2}$-symmetry of the order parameter has been predicted by Hu [6]. These zero energy Andreev bound states can be probed by ab-plane tunneling spectroscopy and manifest themselves as a zero bias conductance peak. That is, the presence of Andreev bound states at zero energy represents definite evidence that the order parameter of the investigated superconductor changes sign along the Fermi surface. We emphasize that the same π phase shift in the Josephson interference experiments by Tsuei *et al.* [4] is the origin of the Andreev bound states and the zero bias conductance peak in the ab-plane tunneling conductance.

In this article we present comprehensive experimental data on ab-plane tunneling spectroscopy for various HTS materials. The data have been obtained using [001] tilt HTS grain boundary Josephson junctions (GBJs). In contrast to low temperature scanning tunneling spectroscopy and experiments using SIN-type planar junctions, GBJs represent superconductor-insulator-superconductor (SIS) Josephson junctions [7,8,9]. An important advantage of the use of GBJs as compared to low temperature scanning tunneling spectroscopy is the very good long term stability of GBJs which allows for the detailed study of the temperature and magnetic field dependence of the tunneling spectra. Furthermore, in GBJs one deals with internal surfaces or interfaces. This implies that degradation or contamination effects due to *ex situ* processing in ambient atmosphere are of minor importance. Only oxygen depletion in the region of the grain boundary can occur, but to a less extent as compared to bare surfaces used in low temperature scanning tunneling spectroscopy experiments. The tunneling data of the recent experiments using SIN-type junctions could be consistently explained by the formation of Andreev bound states as a consequence of a dominating d-wave symmetry of the order parameter in the investigated HTS materials [10,11,12,13]. Here, we show that the same is true for the SIS-type GBJs fabricated from different HTS materials. Our experimental results can be compared to recent theoretical predictions by Barash *et al.* [14] and Tanaka *et al.* [15] on the Josephson behaviour of junctions with d-wave electrodes. Our detailed experimental study clearly shows that the zero bias conductance peak observed in HTS-GBJs is caused by Andreev bound states. Competing explanations for the origin of the zero bias conductance peak, in particular the magnetic scattering scenario, which is based on a model by Anderson and Appelbaum [16,17] developed for NIN-type junctions containing magnetic impurity states, can be ruled out.

Our analysis includes tunneling data obtained for the three hole doped HTS materials $YBa_2Cu_3O_{7-\delta}$ (YBCO), $Bi_2Sr_2CaCu_2O_{8+\delta}$ (BSCCO), and $La_{2-x}Sr_xCuO_4$ (LSCO). Here, YBCO has been investigated in the optimum doped phase with a critical temperature T_c of 90 K and in the underdoped phase with a T_c of about 60 K. Furthermore, the electron doped material NCCO has been studied. The analysis of this material is of particular interest with respect to the question whether or not there is a change in sign of the order parameter for NCCO. Up to now, there is convincing experimental evidence that NCCO has a dominating s-wave symmetry of the order parameter [18,19,20,21], i.e., the order parameter of NCCO is expected to show no change in sign for different k-directions. Hence, Andreev bound states are expected only for hole doped HTS, which are believed to have a dominating d-wave symmetry of the order parameter, but should be absent for NCCO. As we shall see below, this is indeed the case [21,22].

2 Theoretical background

There are several theoretical models that can account for a zero bias conductance peak in the tunneling spectra of SIN- or SIS-type junctions [23]. Beyond the ABS scenario, the Appelbaum-Anderson model and the Blonder-Tinkham-Klapwijk model, phase diffusion in HTS Josephson junctions has been discussed [24,25]. However, any conductance peak related to a supercurrent should be restricted to a much smaller voltage scale than the mV-scale usually measured for the zero bias conductance peak in most experiments. Moreover, any model based on supercurrents fails for SIN-type junctions. In the following we therefore will restrict our discussion to the Appelbaum-Anderson model, , the Andreev bound state model, and the Blonder-Tinkham-Klapwijk model.

2.1 Appelbaum-Anderson model

Zero-bias anomalies in the conductance of normal metal-insulator-normal metal (NIN) tunnel junctions often have been observed and can have various reasons [26,27]. In a model developed by Appelbaum and Anderson it is assumed, that the tunneling barrier is associated with localized paramagnetic states [16,17]. The tunneling conduction electrons are exchange coupled to these states leading to exchange scattering off the localized states. Similar to the $s - d$ interaction model giving a resistance minimum in dilute magnetic alloys (Kondo-type scattering [28]), the Appelbaum-Anderson model can account for a zero bias conductance peak. The tunneling conductance G in the Appelbaum-Anderson model is given by three terms $G = G_1 + G_2 + G_3$, where G_1 is the contribution from all tunneling processes without spin interaction. G_2 is the spin exchange process contribution to the conductance that, of course, depends on the applied magnetic field but not on the voltage at zero field. G_3 is the Kondo-type contribution where an electron is scattered by the exchange interaction leading to the interference of reflected

and transmitted waves. This additional tunneling channel contributes logarithmically to the conductance as

$$G_3(V, T) \propto \ln\left(\frac{E_0}{|eV| + nk_BT}\right). \qquad (1)$$

Here, E_0 is an energy cut-off and n a factor close to unity. An applied magnetic field H results in a Zeeman splitting of the impurtiy states. Then, G_2 is strongly suppressed for quasiparticle energies eV smaller than the distance between the Zeeman-levels and rises abruptly for $|eV| \geq g\mu_BH$, where g is the Landé g-factor, and μ_B the Bohr magneton. Furthermore, G_3 is splitted by $2\delta = 2g\mu_BH$. Strictly speaking, G_3 splits into three peaks with one peak centered at zero-bias. However, the spectral weight of this peak goes to zero as δ is increased, probably impeding the measurement of this zero-energy peak [16].

The Appelbaum-Anderson model has been successfully applied to Josephson tunnel junctions formed by low-temperature superconductors employing hydrogenated amorphous silicon barriers [29]. Initially, it also was used to explain the experimentally observed zero bias conductance peak in tunnel junctions employing HTS electrodes [12,30,31,32,33,34]. However, as will be shown below the Appelbaum-Anderson model cannot account for the temperature and magnetic field dependence of the zero bias conductance peak observed for the HTS junctions including the GBJs. We emphasize that in general localized magnetic states in superconductors can lead to bound states within the gap as pointed out long ago by Zittartz *et al.* [35].

2.2 Andreev bound state model

The formation of Andreev bound states or midgap surface states in high temperature superconductors having zero energy with respect to the Fermi energy and sizable areal density as a consequence of a $d_{x^2-y^2}$-symmetry of the order parameter has been predicted by Hu [6]. The spectral weight of these bound states has a maximum for (110) oriented surfaces, whereas no such states are expected for (100) or (010) surfaces. That is, the mid gap states exist for any specular surface except for the lobe direction of the $d_{x^2-y^2}$-gap perpendicular to the surface. The physical reason for the midgap states is the fact that quasiparticles reflecting from the surface experience a change in the sign of the order parameter along their classical trajectory and subsequently undergo Andreev reflection. Constructive interference of incident and Andreev reflected quasiparticles result in bound states confined to the surface. That is, the midgap states can be understood in terms of Andreev reflections, where the quasiparticle changes from particle-like to hole-like and *vice versa*, and $\mathbf{k}$ changes sign [36,37]. Therefore, the midgap states also are denoted as Andreev bound states. Reversal of the velocity by Andreev reflection always is accompanied by a change in sign of the charge. Consequently, Andreev bound states can carry current, where current conservation is maintained by conversion of the bound state current to supercurrent

far away from the surface. The Andreev bound states result in a zero bias conductance peak in an *ab*-plane tunneling spectrum. Thus, methods that probe the quasiparticle current on a surface or through an interface represent phase sensitive methods in the sense that the existence of Andreev bound states gives definite information on a change in sign of the pair potential. Hence, tunneling spectroscopy becomes a valuable phase sensitive technique for probing the symmetry of the order parameter in HTS.

The basic mechanism required to understand the formation of surface or interface bound states in $d_{x^2-y^2}$-HTS is the process of Andreev reflection [36]. In general, Andreev reflection always plays a role if there is a variation of the order parameter along the classical trajectory of a quasiparticle. That is, Andreev reflection can be viewed as scattering induced by spatial variations of the order parameter. Such variations of the order parameter are well known for interfaces in artificial layer structures such as NS-interfaces. However, they also can occur along the trajectory of quasiparticles specularly reflected at the surface of a superconductor having a spatially anisotropic order parameter. In the process of Andreev reflection a particle-like excitation undergoes branch conversion into a hole-like excitation with reversed group velocity and *vice versa*. In order to discuss the importance of Andreev reflection for the formation of Andreev bound states at surfaces and interfaces of HTS in more detail let us consider the situation shown by Fig. 1(a). An incident quasiparticle with a k-vector corresponding to the negative lobe of the pair potential reflects specularly off the surface. For simplicity, a (110) surface ($\alpha = \pi/4$) and a quasiparticle that is incident under an angle β is considered. The order parameter $\Delta(\mathbf{k}, \mathbf{r})$ experienced by the quasiparticle is a function of momentum $\mathbf{k}$ and space $\mathbf{r}$. It is evident that incident and reflected wave packets propagate through different order parameter fields. For the situation shown in Fig. 1(a) the order parameter has different sign for the incident and reflected wave packet. This is shown more clearly in Fig. 1(b), where we have plotted the order parameter field along the classical trajectory of the quasiparticle. The rounding of Δ close to the surface is due to pair-breaking effects and plays no role for the formation of Andreev bound states. However, it becomes important if pair breaking frees significant spectral weight for subdominant pairing channels as will be discussed in section 2.3.

In general, Andreev bound states occur at energies for which the phases of Andreev reflected particle-like and hole-like excitations interfere constructively. According to the Atiyah-Singer index theorem zero energy bound states are always formed, if the scattering induces a change in sign of the order parameter along the classical trajectory [38]. For the situation shown in Fig. 1 this is always directly at the interface ($d = 0$). Thus, changing the incident angle β will not change the location of the Andreev bound states at $d = 0$. Reducing α from $\pi/4$ towards $\alpha = 0$ results in a increasingly smaller range of incident angles β for which a change in sign of the order parameter field is obtained. Thus, the spectral weight of the zero energy bound states decreases with decreasing α and vanishes for
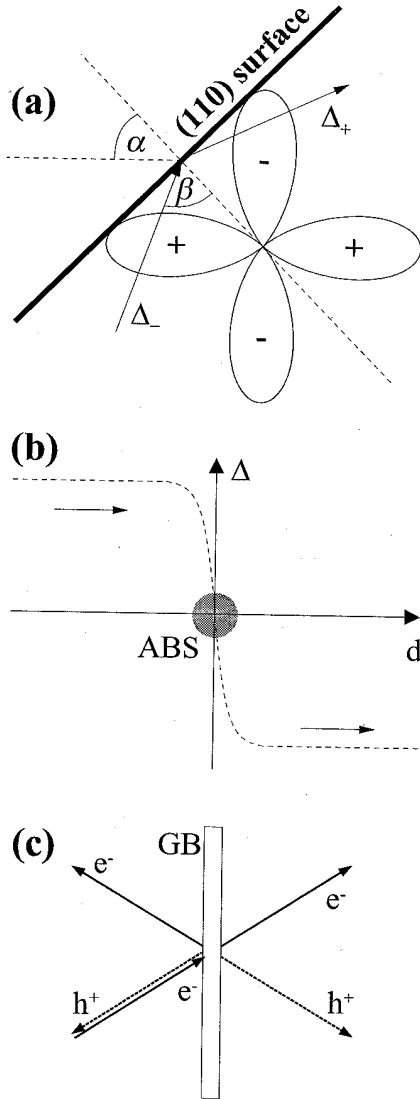
Fig. 1. Formation of Andreev bound states: In (a) a mixed real/momentum space representation is shown for a (110) oriented surface of a HTS having a $d_{x^2-y^2}$ symmetry of the order parameter. The propagation direction of the quasiparticle is indicated by the arrows and can be transferred to a direction in k-space by plotting a **k**-vector from the origin of the lobe to its edge parallel to the propagation direction in real space. In (b) the order parameter Δ is plotted versus the path d along the quasiparticle trajectory. For the case of a sign change on reflection the Andreev bound states are always formed at the surface ($d = 0$). In (c) a schematic illustration of the different reflection and transmission processes of quasiparticles at a grain boundary (GB) interface is given.

$\alpha = 0$, i.e. for a (100) or (010) oriented surface. That is, the spectral weight of the Andreev bound states is largest for (110) surfaces and decreases continously towards zero for (100) or (010) surfaces. It is evident that for trajectories orthogonal to the CuO_2-plane no Andreev bound states are formed.

Above we have considered the situation present at the surface of a HTS. We now briefly discuss the situation for a SIS-structure present for the GBJs studied in our experiments. In Fig. 1(c) the possible transmission and reflection processes at a grain boundary interface are shown schematically. An incident particle-like excitation is injected from the left bulk d-wave HTS under a finite angle with respect to the grain boundary plane. Discussing the reflection processes, the particle-like excitation can be either specularly or Andreev reflected. In the latter case it is turned into a hole-like excitation propagating in opposite direction. In the same way, transmission through the insulating grain boundary barrier can yield particle- and hole-like excitations. As described above for the case of reflection at a surface, the quasiparticles involved in the different reflection and transmission processes experience different pair potentials depending on their k-vector and the relative orientation of the order parameter in both electrodes with respect to the grain boundary barrier in both electrodes. We also note that Cooper-pairs have to be involved to establish charge conservation.

We point out that different order parameter symmetries will produce different k-dependencies of the spectral weight of Andreev bound states. Of course, Andreev bound states are present only if there is a change in sign of the pair potential in different k-directions and are absent if there is none. For example, for a d_{xy}- and $d_{x^2-y^2}$-symmetry the maximum spectral weight of the Andreev bound states is obtained for a (100) or (110) oriented surface or interface, respectively. In contrast, for a s-wave symmetry no sign change of the order parameter and, hence, no Andreev bound states are present. Thus, the experimental observation of Andreev bound states gives definite evidence for an order parameter changing sign on the Fermi surface and represents a phase sensitive probing technique. In cases where the order parameter symmetry is not fully established, as for example for the electron doped NCCO, Andreev bound states sensitive experiments can be used to clarify whether or not the order parameter changes sign in different k-directions.

2.3 Consequences of the Andreev bound state model

There are several new and interesting phenomena that are directly related to the existence of Andreev bound states at surfaces and interfaces of HTS that will be addressed in the following. So far, there is significant experimental evidence only for the zero bias conductance peak in tunneling data due to Andreev bound states. However, other effects like an anomalous temperature dependence of the critical current of HTS Josephson junctions or an anomalous temperature dependence of the London penetration depth due to "anti-Meissner" currents have not yet been experimentally confirmed.

2.3.1 Zero bias conductance peak

Since Andreev bound states can carry current the most evident experimental consequence is that they should pro-

duce a pronounced zero bias conductance peak in the *ab*-plane tunneling conduction of experiments involving at least one *d*-wave HTS electrode. For the interpretation of the conductance of superconductor-insulator-normal metal (SIN) junctions that can be formed by using a normal metal tip in low temperature scanning tunneling spectroscopy, several groups extended the calculations by Hu [6]. In particular, expressions for the density of states and the conductance of such junctions employing *d*-wave HTS have been derived [14,15,39,40,41,42]. The most prominent feature in the calculated conductance versus voltage curves indeed was a pronounced zero bias conductance peak as a direct consequence of the Andreev bound states. Recently, these states also have been observed experimentally using low temperature scanning tunneling spectroscopy [10,43,44], in particular on well defined (110) oriented HTS surfaces [11]. We note that Andreev bound states are absent at surfaces perpendicular to the *c*-axis direction. Therefore, no zero bias conductance peak has been observed by Renner *et al.* in low temperature scanning tunneling spectroscopy experiments performed on (001) oriented surfaces [45,46,47]. A further possibility for the realization of SIN-junctions is the formation of planar junctions using a normal metal and a HTS electrode separated by a thin insulating layer. Also for such junctions a zero bias conductance peak has been observed in most experiments [12,13,30,31,32,48]. Up to now the theoretically predicted zero bias conductance peak has been found for both SIN- and SIS-type junctions [25,49,50,51]. Below we present comprehensive experimental data on the tunneling conductance of various high temperature superconducting GBJs giving a very complete view of the zero bias conductance peak as a consequence of Andreev bound states. We note that non zero-energy states are also possible as a consequence of a suppression of the order parameter at the surface [42].

2.3.2 Surface roughness

In our discussion of the Andreev bound state model we always have assumed perfectly flat surfaces and interfaces that usually are not present in any experimental situation. The spectral weight of the Andreev bound states and, hence, the measured zero bias conductance peak is very sensitive to surface roughness on a length scale larger than the coherence length. Since the coherence length of HTS is of the order of 1 nm, almost all surfaces can be considered rough. The influence of surface roughness has been theoretically calculated by several authors [42,52,53,54]. The basic consequence of surface roughness is that one has to average over different surface orientations. As a consequence, for a $d_{x^2-y^2}$-symmetry of the order parameter and a (110) oriented surface, for which the spectral weight of the Andreev bound states is maximum, the zero bias conductance peak is suppressed by surface roughness. *Vice versa*, a finite zero bias conductance peak can appear for (100), (010), and (001) surfaces and interfaces due to surface roughness. That is, surface roughness smears out the pronounced dependence of the Andreev bound states
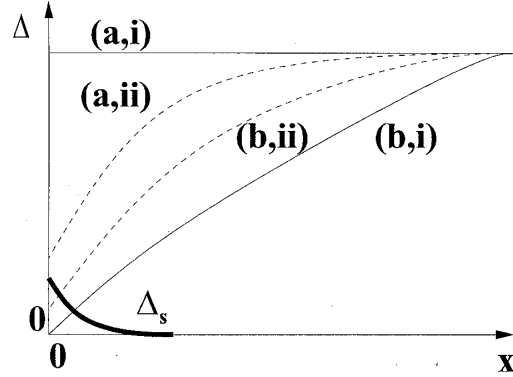

Fig. 2. Qualitative plot of the amplitude of the order parameter as a function of the distance from the surface for a (100) (a) and (110) (b) surface without (i) and with (ii) surface roughness, respectively. Also shown is a surface induced *s*-wave order parameter that can be obtained for a (110) surface by surface pair breaking effects for the dominant *d*-wave and subsequent pairing into the subdominant *s*-wave channel.

spectral weight on the relative orientation of the surface and the order parameter. As an example, in Fig. 2 the order parameter is plotted versus the distance from the surface for smooth and rough surfaces with different orientation. It is evident that due to surface roughness differently oriented surfaces behave in a similar way. This makes it experimentally more difficult to distinguish the different directions within the superconducting plane. However, since the sign change of the pair potential is a necessary prerequisite for the formation of Andreev bound states, any amount of surface roughness can not produce a zero bias conductance peak for an order parameter having no sign change on the Fermi surface such as an *s*-wave order parameter.

2.3.3 Anomalous temperature dependence of the Josephson current density

A further important consequence of the Andreev bound states is an anomalous behaviour of the temperature dependence of the maximum Josephson current I_c at low temperatures [55,56]. Recently, is was predicted by Tanaka and Kashiwaya [55] that for a fixed phase difference between the electrodes of a Josephson junction formed by *d*-wave superconductors the supercurrent across the junction can be either positive or negative depending on the injection angle of the quasiparicles. Loosly speaking, the junction can be thought as a combination of so-called 0- and π-junctions. Due to different temperature dependencies of both components of the critical current, this may result in a nonmonotonous temperature dependence of the Josephson current. In particular, such behaviour is expected for symmetric [001] tilt HTS grain boundary junctions. We point out that this feature is expected only when Andreev bound states are formed at the interface of

both junction electrodes and if there is a change in sign of the Josephson current as a function of injection angle. The predicted nonmonotonous $I_c(T)$ is in clear contrast to the behaviour of traditional Josephson junctions formed by s-wave superconductor, for which a monotonous increase of I_c with decreasing temperature is theoretically predicted and experimentally observed. The nonmonotonous $I_c(T)$ dependence for d-wave Josephson junctions again is sensitive to interface roughness. For increasing roughness the anomaly is shifted to lower temperatures [56]. This may be the reason why this effect has not yet been convincingly experimentally observed. Additionally, the presence of a subdominant s-wave component of the order parameter as discussed in the next section is predicted to suppress strongly the enhancement of the Josephson current at low temperatures [57].

2.3.4 Splitting of the zero bias conductance peak by a broken time reversal symmetry state

It has been shown in general that a locally time reversal symmetry breaking state at interfaces of unconventional superconductors can exist that decays exponentially toward the bulk [58]. In a broken time reversal symmetry state the Andreev bound states shift to finite energy resulting in a split zero bias conductance peak. A broken time reversal symmetry state is obtained by applying a magnetic field. However, even at zero applied magnetic field time reversal symmetry can be broken by the presence of two order parameters at the surface having a $\pi/2$ relative phase difference. The possible coexistence of a second order parameter with s-wave symmetry that can become stable at surfaces of HTS but is completely dominated by the d-wave potential in the bulk material has been discussed by Sigrist et al. [58] and Matsumoto et al. [52]. Such situation is possible at the surface of a d-wave HTS, since the surface may act as strong pair breaker for the d-wave paired quasiparticles thereby releasing spectral weight for the formation of pairs in a subdominant (e.g. s-wave) pairing channel. Below a surface transition temperature then a surface order parameter can develop that spontaneously breaks time reversal symmetry and results in spontaneous surface currents. The pairing symmetry at the surface can be a mixed $d + is$ (or in another notation $B_{1g} + iA_{2g}$) phase. Note that both order parameters coexist at the surface with a relative phase shift of $\pi/2$ that leads to a spontaneous surface current. The Andreev bound states then are shifted to finite energy due to the Doppler shift $\mathbf{v}_f \cdot \mathbf{p_s}$, where $\mathbf{p_s}$ is the condensate momentum due to the spontaneous supercurrent. This in turn leads to a split zero bias conductance peak in zero applied magnetic field [59,60]. That is, the measurement of the conductance in ab-plane tunneling experiments can give information on the presence of a surface order parameter in HTS that spontaneously breaks time reversal symmetry. Recently, this effect has been found to be consistent with the $t - J$-model [61] in the case of sufficiently large J at the surface of a d-wave superconductor [62,63].

Recently, a zero field splitting and a nonlinear evolution of the magnitude of the splitting with increasing applied magnetic field as predicted by Fogelström et al. [59], has been reported for planar SIN-junctions [13,31] and for low temperature scanning tunneling spectroscopy experiments [64].

2.3.5 Anomalous Meissner current

The London-penetration depth λ_L of a superconductor is known to be related to the density of paired quasiparticles. For the different symmetries of the order parameter a different behaviour of $\lambda_L(T)$ has been predicted and experimentally found [65,66,67]. The presence of Andreev bound states at surfaces of HTS can have a significant effect on the low temperature dependence of the London penetration depth. In order to clarify this effect let us consider the surface of a d-wave superconductor where Andreev bound states are formed. In a state with established time reversal symmetry there is no net current parallel to the surface, since in thermal equilibrium the contributions of all Andreev bound states exactly cancel each other. However, applying a magnetic field parallel to the surface results in a broken time reversal symmetry state and a Meissner shielding current. This in turn results in a Doppler shift $\mathbf{v}_f \cdot \mathbf{p}_s$, where $\mathbf{p_s}$ now is the condensate momentum due to the Meissner shielding current. Since the Doppler shift has opposite sign for Andreev bound states with opposite v_f, in thermal equilibrium there is no longer an equal population of states with opposite v_f. This results in a net surface current that is opposite to the usual Meissner shielding current and therefore is denoted as "anti-Meissner" current. In contrast to the usual Meissner shielding current flowing in a surface layer of depth λ_L, this "anti-Meissner" current flows in a surface layer given by the ab-plane coherence length ξ_{ab}. It becomes important at low temperatures where is causes an anomalous temperature dependence of the London penetration depth $\lambda_L(T)$ [68]. Due to the "anti-Meissner" current the London penetration depth is slightly increased beyond the value expected without this current. First experimental evidence for this effect has been reported recently by Walter et al. [69] and more evidence will be presented below for HTS-GBJs.

2.4 Blonder-Tinkham-Klapwijk model

Blonder, Tinkham, and Klapwijk (BTK) developed a generalized Andreev reflection model for junctions involving superconductor-normal metal (S/N) interfaces [70,71]. To account for a finite barrier strength at the S/N interface they introduced a dimensionless factor Z. For example, in the limiting case of $Z = 0$ the transmission coefficient of the junction that is given as $1/(1 + Z^2)$ becomes unity. In the $Z = 0$ limit and for small values of Z the BTK model predicts a peak in the normalized differential conductance at zero voltage that reaches a maximum value of 2. This peak decreases monotonously with increasing voltage, that is, the BTK model predicts a conductance peak

at zero bias. However, no gap structure in the conductance versus voltage curves is expected to be observed for small Z. That is, within the BTK-model the observation of both a gap like structure *and* a zero bias conductance peak is not expected. We emphasize that the BTK-model was developed for conventional BCS superconductors. Therefore, in its original form the BTK-model is not sufficient to explain the experimentally observed tunneling spectra of d-wave superconductors. However, the BTK-model can be used as a starting point for more elaborate theories. The Andreev bound state model represents a generalized BTK-type model that accounts for an arbitrary Z and an anisotropic pair potential.

3 Experimental Results

3.1 Sample preparation and experimental techniques

In our experiments both symmetric ($\alpha_1 = -\alpha_2$) and asymmetric ($\alpha_1 = 0$; α_2) [001] tilt HTS-GBJs fabricated on SrTiO$_3$ bicrystal substrates were used. A sketch of the grain boundary junction geometry is shown in Fig. 3. The symmetric GBJs had a total misorientation angle ($\alpha_1 + \alpha_2$) of 24° and 36.8°, for the asymmetric [001] tilt GBJs we used $\alpha_2 = 45°$. Only c-axis oriented epitaxial thin films were grown on the bicrystal substrates. In this way the tunneling direction in the grain boundary junction configurations always is along the ab-plane. The YBCO thin films were deposited using both hollow cathode magnetron sputtering and pulsed laser deposition from stoichiometric targets. YBa$_2$Cu$_3$O$_{7-\delta}$ samples were fabricated with different oxygen content. Both fully oxidized YBCO with a critical temperature T_c of about 90 K and oxygen deficient YBCO with T_c values ranging between 55 and 60 K were used. We note that the T_c reduction in the oxygen deficient YBCO is obtained by well controlled oxygen depletion and is not caused by the presence of magnetic impurities in the samples or at the grain boundary. Furthermore, BSCCO-GBJs were fabricated in the same way with a T_c of the BSCCO-films of about 80 K [72]. This T_c value is reduced by about 10 K as compared to optimum doped samples [73]. The epitaxial LSCO thin films have been grown on the bicrystal substrates by reactive coevaporation from metal sources using ozone as reaction gas [74,75,76]. The T_c of these samples typically was about 24 K. This value is comparable to other epitaxial thin film samples but slightly reduced compared to that of the best single crystals of LSCO. This most likely is due to strain at the interface between the substrate and the epitaxial thin film [76,77]. Finally, the NCCO films were deposited similar to the LSCO films by molecular beam epitaxy (MBE) using ozone as oxidation gas [74]. The T_c of about 24 K is one of the highest reported for this material in literature including even NCCO single crystals [78]. After their growth, the HTS thin film bicrystals have been patterned using optical lithography and Ar ion beam etching to obtain a GBJ structure as sketched in Fig. 3.

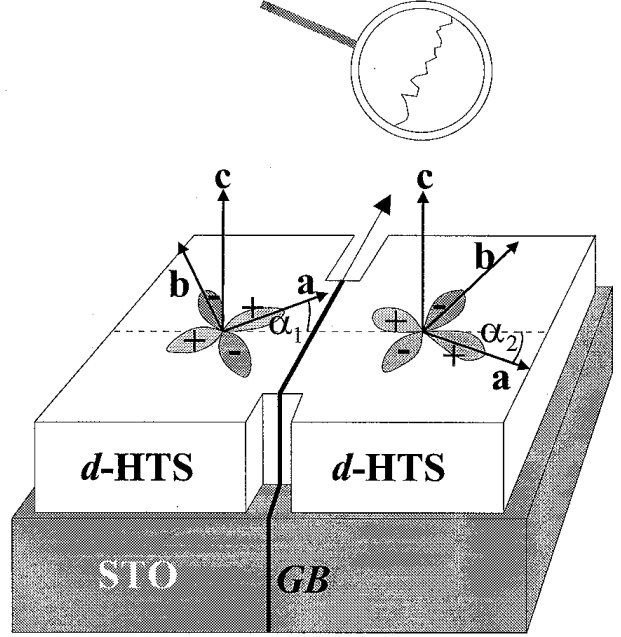The measurements of the current-voltage [$I(V)$] and conductance vs. voltage [$G(V) = dI(V)/dV$] characteris-

Fig. 3. Sketch of the sample geometry of a symmetric [001] tilt HTS-GBJ. The crystal axis **a**, **b**, and **c** and the misorientation angles α_1 and α_2 are indicated. For a symmetric and asymmetric junction we have $\alpha_1 = -\alpha_2$ and $|\alpha_1| \neq |\alpha_2|$, respectively. Also given is a magnified view of the grain boundary microstructure indicating the strong faceting of the grain boundary. The nominal misorientation angle is only the average angle of a wide range of different angles of the individual facets.

tics were performed in a standard four-probe arrangement. If necessary the critical current was suppressed by applying a small magnetic field parallel to the grain boundary plane corresponding to a minimum in I_c vs. H. Zero field measurements were performed in magnetically shielded cryostats placed in an rf-shielded room. Also, high magnetic fields up to 12 T and low temperatures down to 100 mK were used in our study.

3.2 Transport mechanism in GBJs

The electrical transport properties of grain boundaries in the cuprate superconductors have been studied intensively over the last years. Recent reviews have been given by Gross *et al.* [7,9]. Here, we briefly summarize the main results relevant to the tunneling spectroscopy experiments discussed below. Phenomenologically, the superconducting properties of the GBJs can be well modeled by the resistively and capacitively shunted junction (RCSJ) model [7,79]. In order to describe the vaste majority of the present experimental data on the electrical transport and noise properites of HTS-GBJs the intrinsically shunted junction (ISJ) model has been suggested [80,81]. In this model it is assumed that there is a thin insulating grain boundary barrier containing a large density of localized defect states.

The microscopic transport mechanism then is direct and resonant tunneling via the localized states. A key feature of the ISJ-model is the fact that the transport of Cooper pairs via the localized states is prevented by Coulomb repulsion, i.e. Cooper pairs have to use the direct tunneling channel, whereas due to the large density of defect states the quasiparticle transport is dominated by resonant tunneling via a single localized state [73,82,83,84,85,86,87]. The resonant channel can be viewed as to provide an intrinsic resistive shunt leading to the name intrinsically shunted junction. The ISJ-model well explains the scaling behaviour $V_c = J_c \rho_n \propto (J_c)^q$ with $q \sim 0.5$ observed for the GBJs [80,88]. Here, J_c and ρ_n are the critical current density and the normal resistance times area of the GBJ. Furthermore, it naturally accounts for the large amount of low frequency excess noise due to trapping and release of charge carriers within the localized states [73,86].

We emphasize that the tunneling processes present in GBJs are elastic processes. If inelastic transport processes would be important, a significant temperature dependence of the tunneling conductance for voltages well above the gap voltage would be expected. However, the experimental data on GBJs show a temperature independent conductance [34]; i. e. inelastic tunneling via two and more localized centers is negligible. Hence, the tunneling quasiparticles can carry spectroscopic information on the density of states (DOS) in the junction electrodes and thereby e.g. on the energy gap. In contrast, such spectroscopic information is destroyed, if multistep inelastic tunneling or even variable range hopping would be the dominating transport process. We also note that the localized states within the grain boundary barrier have an about white energy distribution. Hence, they do not act as an energy filter producing structures in the conductance versus voltage curves of HTS-GBJs. Because all junctions used in our experiments could be well fitted within the above picture, we assume that the same tunneling mechanism is present in all investigated junctions.

There have been extensive studies on the microstructure of the grain boundary barrier. High resolution transmission electron microscopy (HRTEM) revealed a strongly faceted grain boundary barrier with facets on a nanoscale [89]. This means that the macroscopic misorientation angles α_1 and α_2 of the grain boundary, which are determined by the bicrystal substrate, represent average values only. However, on a microscopic scale these angles can vary considerably due to the faceting with $|\alpha_1| + |\alpha_2| = const.$ As a consequence in some cases GBJs formed by d-wave HTS materials have to be modelled as a parallel array of so-called "0"- and "π"-junctions showing an irregular magnetic field dependence of the critical current [90,91]. This effect is negligible for symmetric GBJs with small misorientation angles ($|\alpha_1| + |\alpha_2| < 25°$) [87], however, it becomes more pronounced for increasing misorientation angle and stronger faceting. In general, the faceted grain boundary barrier can be viewed as a rough interface. The impact of surface roughness on the spectral weight of Andreev bound states on their consequences already has been discussed above. Unfortunately, up to now no exact
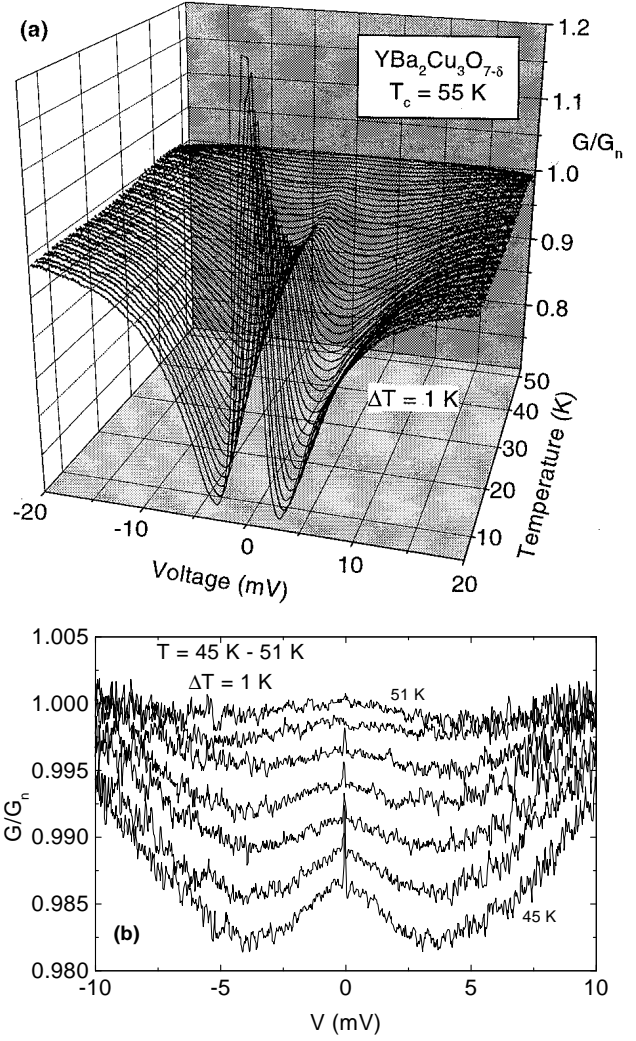

Fig. 4. (a) Normalized differential conductance vs. voltage for a 24° [001] tilt YBCO-GBJ for temperatures between 4 and 51 K. The sample was underdoped with $T_c \approx 55$ K. Some data points close to zero are removed because of the Josephson current peak. (b) The same dependence for temperatures between 45 and 51 K on an enlarged scale. One clearly can distinguish the sharp Josephson current peak at zero bias, the much broader zero bias conductance peak, and the superconducting gap structure even for T close to T_c.

quantitative description of the effects of a faceted grain boundary on the electrical transport properties is available. Below we will qualitatively discuss possible effects of the faceting that can be understood from simple angle averaging.

3.3 Tunneling spectroscopy of HTS-GBJs

In this section we present our experimental results on the tunneling spectroscopy on various HTS materials using GBJs. In the next section we will discuss in detail our

results in the framework of the different models discussed above.

We first consider the conductance versus voltage curves of the hole doped HTS YBCO, BSCCO, and LSCO, which are believed to have a d-wave symmetry of the order parameter. Fig. 4a shows a set of typical $G(V)$-curves normalized to the normal state conductance G_n. The curves were obtained for a $24°$ [001] tilt YBCO-GBJ at temperatures ranging between 4 and 51 K. The Josephson current peak at zero voltage has been removed for clarity. The sample of Fig. 4a was underdoped and had a T_c of about 55 K. In Fig. 4b some spectra are shown on an enlarged scale in order to better show the presence of the broad zero bias conductance peak up to the T_c of the material. Furthermore, the superconducting gap structure and a narrow peak at $V = 0$ due to the Josephson current can be observed up to T_c. For other hole doped HTS materials such as BSCCO and LSCO the same behaviour was observed. For LSCO with $T_c \approx 24$ K the experimental results have been published recently [92]. For all samples the zero bias conductance peak is found to decrease with increasing temperature and to disappear at T_c. Furthermore, also the gap structure is found to disappear at T_c.

The measured tunneling spectra are almost perfectly symmetric about zero voltage as expected for a symmetrical tunnel junction with electrodes formed by the same material. Far above the gap voltage the conductance was found to be independent on temperature and has an about parabolic shape [85]. The parabolic shape can be explained by the effect of the applied voltage on the shape of the barrier potential. The background conductance can be viewed as normal state conductance G_n. In order to show the temperature dependence of the spectra more clearly, the conductance data have been normalized with respect to G_n. Fig. 4 clearly shows that below the gap voltage the density of states is reduced by about 30%. With increasing temperature the conductance smoothly merges towards to the normal state conductance when the temperature is approaching T_c. Recently, Ekin *et al.* [22] reported the disappearance of the zero bias conductance peak at temperatures well below the transition temperature of the material. Such behaviour has not been observed in our study and thus might be an effect of sample fabrication. In our case a clear correlation between the appearance of a measurable zero bias conductance peak and T_c was observed.

The materials we used for our experiments were both hole doped HTS (60 and 90 K phase of YBCO, BSCCO, and LSCO) and an electron doped HTS (NCCO). We now compare the data of the hole doped HTS to that obtained for the electron doped HTS. There is significant experimental evidence that the hole doped materials have a d-wave symmetry of the order parameter, whereas NCCO has a dominating s-wave component. From our experiments on GBJs fabricated from these materials we can conclude that all hole doped HTS show a pronounced zero bias conductance peak, whereas such peak is completely absent for the electron doped NCCO. In order to demonstrate this observation, in Fig. 5 we show data for fully oxidized YBCO, as well as for LSCO and NCCO. Again
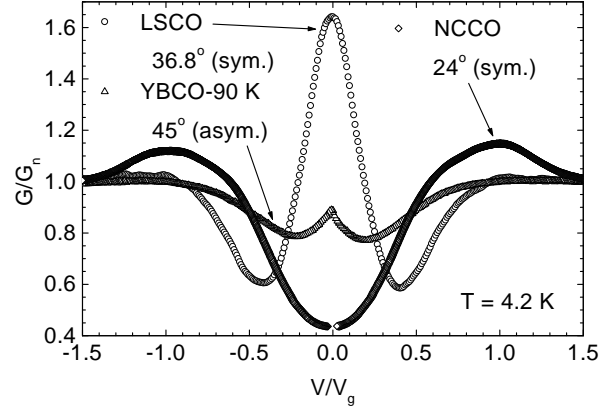

Fig. 5. Normalized conductance vs. normalized voltage of GBJs formed by LSCO, YBCO (90 K phase), and NCCO. The YBCO-GBJ was an asymmetric [001] tilt GBJ while the LSCO- and NCCO-GBJ were symmetric [001] tilt GBJs. For the NCCO-GBJ the Josephson current peak has been removed.

the data is normalized to the normal conductance G_n. Furthermore, the voltage scale is normalized to the gap voltage V_g in order to compare data of materials with different gap values. Here, we have chosen $V_g = \Delta_0/e$ and not, as for tunnel junction using conventional BCS-like superconductors, $V_g = 2\Delta_0/e$. We also note that the exact position of the conductance peak due to the gap depends on the orientation of the electrodes with respect to the barrier. This is a consequence of the (interface) density of states in a d-wave superconductor [14]. In general, the same consideration should apply for a highly anisotropic s-wave superconductor. Therefore, in a first order approximation $V_g \sim \Delta_0/e$ is assumed for NCCO as well. Typical gap voltages of the different materials were 6 mV for both LSCO and NCCO, 15 mV for the 60 K phase of YBCO (YBCO-60), 20 mV for the 90 K phase (YBCO-90), and 25 mV for BSCCO.

With respect to the gap structure in the measured tunneling spectra we would like to add an interesting observation concerning the magnitude of the gap. As can be seen from Fig. 4a the magnitude of the gap seems to be about constant with increasing temperature. However, the states within the gap are filled up with increasing temperature until the normal state value is reached. Above T_c the presence of a gap could *not* be observed in our experiments. A similar behaviour has been observed by Renner *al.* [46,47] using low temperature scanning tunneling spectroscopy. However, in contrast to our observation these authors report a gap persisting even above T_c. We note, that the tunneling direction in the experiments by Renner *et al.* was along the c-axis, whereas it is along the ab-plane in our study. The observed temperature evolution of the gap structure completely deviates from the BCS-behaviour and is probably related to the pseudogap that has been observed in the HTS [93,94].

We next consider the magnitude of the gap as a function of the doping level. Recently, an increasing gap was found with decreasing doping concentration for BSCCO

[47,95]. In the case of $YBa_2Cu_3O_{7-\delta}$ we investigated the two doping concentrations $\delta \simeq 0$ and $\delta \simeq 0.4$. In contrast to the recent work on BSCCO, we observed a linear scaling of the gap values with T_c. We note, however, that this behaviour has to be examined in more detail in future. Also for NCCO, the gap value was found to scale with T_c. A junction with a T_c of about 14 K had a gap value of about 3.5 meV, whereas junctions with $T_c \simeq 24$ K showed gap values of about 6 meV.

The conductance versus voltage curves of GBJs fabricated from the d-wave HTS [96] all show some common properties. Firstly, they have a pronounced zero bias conductance peak. Secondly, the width of the zero bias conductance peak is always about several mV and is not narrowing with decreasing temperature. Thirdly, the conductance is reduced in an energy range corresponding to the superconducting gap energy most likely due to a reduced density of states. For all d-wave HTS only a reduction of the density of states of about 30 to 50% is observed. Additionally, a broad and flat peak in the $G(V)$ curves is observed at the gap voltage, however, not for all samples. Finally, reducing the temperature to very small values (down to 100 mK) results in a zero bias conductance peak with a shape that is more Lorentzian-like than Gaussian-like. As shown in Fig. 5, a Gaussian shape is obtained for LSCO at 4.2 K, whereas for YBCO-90 already a Lorentzian shape is obtained at this temperature. This indicates that the measured linewidth is not determined by extrinsic effects such as thermal smearing or the finite experimental resolution but represents an intrinsic linewidth of the zero bias conductance peak. Calculating the linewidth of the zero bias conductance peak, an imaginary part can be added to the energy introducing a phenomenological lifetime parameter Γ of the order of $\Delta_0/10$ [11]. Recently, a momentum-dependent intrinsic broadening of the surface bound states has been predicted [97].

The behaviour of NCCO-GBJs differs from that of GBJs fabricated from the d-wave HTS in several features. Firstly, the $G(V)$ curves of optimum doped NCCO-GBJs with a maximum T_c of 24 K show a much clearer peak structure at V_g than those of the d-wave HTS-GBJs. Secondly, the gap structure is more pronounced and the density of states is reduced to about 40% of the normal state value. For a NCCO-GBJ with a reduced T_c both the peak at V_g and the reduction of the density of states becomes smaller. However, up to now no detailed tunneling spectroscopy as a function of doping has been performed. Finally, it is interesting to note that the spectra of NCCO have, apart from the zero bias conductance peak, more similarities to those of the hole doped HTS materials than to those of conventional BCS-superconductors.

We finally consider the magnetic field dependence of the conductance versus voltage curves. The magnetic field dependence of the tunneling spectra of a YBCO-GBJ (60 K phase) is shown in Fig. 6(a). The magnetic field H was applied parallel to the grain boundary barrier in c-axis direction. The magnetic field was increased in 0.5 T steps. In Fig. 6(a) the Josephson current has not been suppressed explaining the sharp spike at zero voltage in the zero field
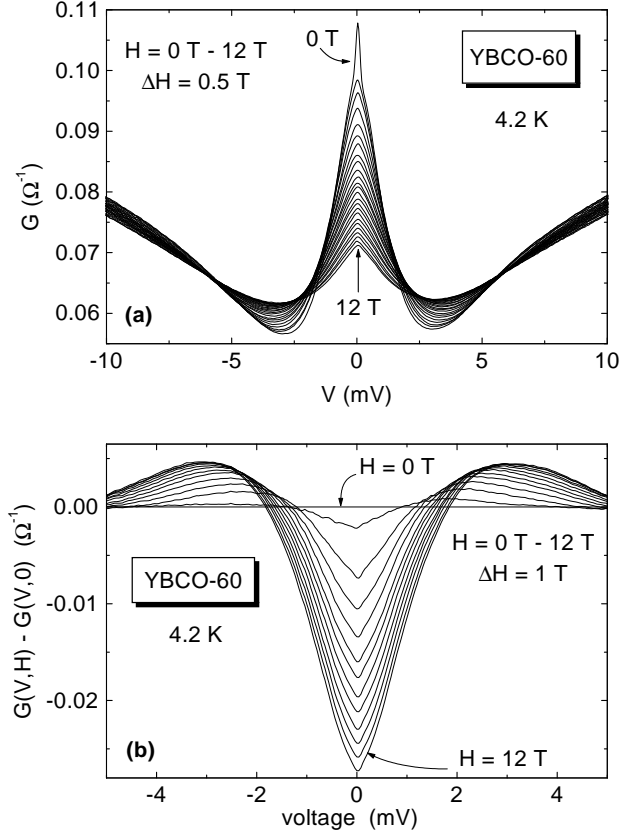

Fig. 6. (a) Magnetic field dependence of the zero bias conductance peak at 4.2 K for a symmetric [001] tilt YBCO-GBJ (60 K phase). In (b) $(G(V,H) - G(V,0))$ is plotted for the same sample. The applied magnetic fields ranged between 0 and 12 T (0.5 T steps).

$G(V)$ curve on top of the much broader zero bias conductance peak caused by the Andreev bound states. The effect of the applied magnetic field is the suppression of spectral weight around zero energy. The spectral weight removed around zero energy is shifted to higher energies about the whole energy range. Hence, in the $G(V,H) - G(V,0)$ vs. voltage curves shown in Fig. 6(b) two peaks appear with the peak position increasing non-linearly with increasing applied magnetic field [85]. We note that the overall spectral weight at 12 T is reduced by about 3% below the value at zero magnetic field if we consider a voltage interval of ± 12 mV. However, it is not likely that the conservation of the number of states is violated but that the missing spectral weight is shifted to even higher energies not contained in the considered voltage interval. For LSCO at 100 mK qualitatively the same result has been obtained [92]. Note that the thermal smearing is only of the order of 10 μeV at 100 mK. This explains that for LSCO the zero bias conductance peak in the conductance vs. voltage curves changes from a Gaussian shape at 4.2 K to Lorentzian shape at 100 mK. In contrast to reference [13] but in accordance to reference [22] no direct splitting of the zero bias conductance peak was found at any applied magnetic field up to 12 T.

3.4 Comparison to low temperature scanning tunneling spectroscopy measurements

In this subsection we briefly compare the results obtained for SIS-type HTS-GBJs to those obtained using low temperature scanning tunneling spectroscopy, where a SIN-configuration is used. A low temperature scanning tunneling spectroscopy study of different HTS materials with different orientations has been given recently by Alff *et al.* [21,98]. Details on the low temperature scanning tunneling spectroscopy technique can be found in [21,98] and in the references cited therein. Typical conductance versus voltage curves obtained by low temperature scanning tunneling spectroscopy are shown in Fig. 7. These curves can directly be compared to those of Fig. 5 obtained from experiments using GBJs. We note that the conductance of the two junction types differs by several orders of magnitude. Whereas one has a typical conductance of 10^{-8} S in low temperature scanning tunneling spectroscopy spectra, the conductance of GBJs ranges between 10^{-1} and 10^{-2} S. However, this difference mainly is caused by the different junction area, which is by several orders of magnitude smaller for low temperature scanning tunneling spectroscopy. The low temperature scanning tunneling spectroscopy data of Fig. 7 were obtained by performing experiments on (110) oriented surfaces of NCCO and YBCO. With respect to the zero bias conductance peak, the same result is obtained as for the GBJs. Again, only YBCO shows a zero bias conductance peak while such peak is completely absent for NCCO. We note that by low temperature scanning tunneling spectroscopy also (100) and (001) oriented surfaces have been probed. Also for these surfaces a zero bias conductance peak never has been observed for NCCO [21]. However, for YBCO in many cases a zero bias conductance peak could be detected for (100) and (001) oriented surfaces. For a (100) oriented surface, where in the ideal case no zero bias conductance peak is expected, this is most likely related to the finite roughness of the surface as discussed in section 2.3. This effect is similar to the observation of zero bias conductance peaks for *a*-axis or even *c*-axis oriented planar junctions.

We also would like to address another detail of the conductance versus voltage curves that are similar for both the SIN junctions used in low temperature scanning tunneling spectroscopy and the SIS-type GBJs. For NCCO the $G(V)$ curves show a more pronounced superconducting gap structure with a density of states that is reduced by about 50% within the gap. In contrast, for YBCO this reduction is smaller and (if at all) at the gap voltage only very faint and broad conductance peaks are observed. Finally, we note that in contrast to the spectra of the GBJs the low temperature scanning tunneling spectroscopy spectra show some asymmetry that is most pronounced in the case of YBCO. This feature has been observed in many spectra using low temperature scanning tunneling spectroscopy [45,99]. So far, it is not clear whether this effect is related to the order parameter symmetry. However, one is led to think in this direction because the asymmetry is absent for NCCO.
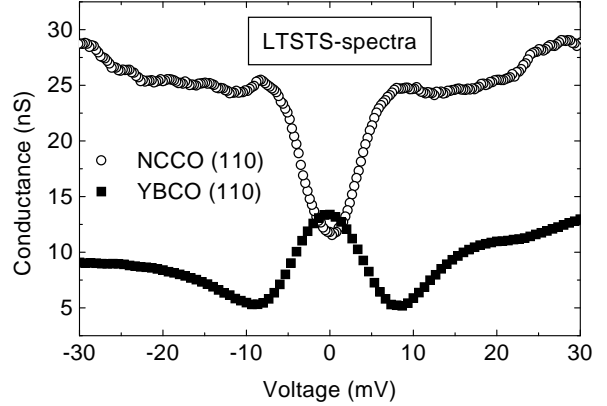

Fig. 7. Low temperature scanning tunneling spectroscopy spectra for (110) oriented surfaces of NCCO and YBCO at 4.2 K. The data are taken from reference [98].

3.5 Anomalous Meissner currents

GBJs formed by different HTS have been successfully used to determine the relative change

$$\frac{\Delta\lambda_{ab}(T)}{\lambda_{ab}(0)} = \frac{\lambda_{ab}(T) - \lambda_{ab}(0)}{\lambda_{ab}(0)}$$

of the in-plane London penetration depth λ_{ab} with the high precision of only a few Å[67]. In this technique the shift of the side-lobes of the $I_c(H)$ dependence of HTS-GBJs is measured as a function of temperature. Details of this precision measurement technique have been described elsewhere [67]. Recently, an anomalous temperature dependence of $\Delta\lambda_{ab}$ was measured for a symmetric $36°$ [001] tilt YBCO-GBJ [100]. As can be seen in Fig. 8, for temperatures below about 10 K the $\Delta\lambda_{ab}(T)/\lambda_{ab}(0)$ dependence shows a clear upturn with decreasing temperature in contradiction to the behaviour expected for a *d*-wave superconductor. We note, that this anomaly can
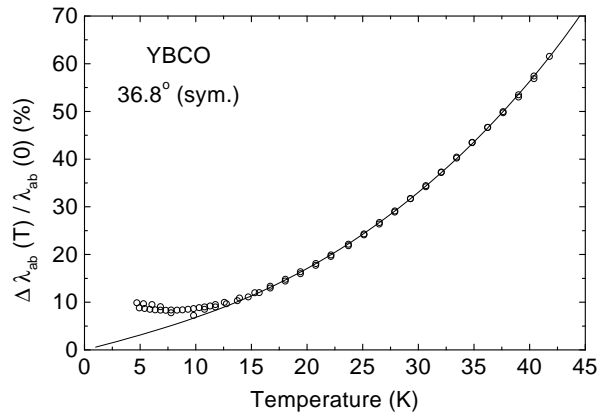

Fig. 8. $[\lambda_{ab}(T)-\lambda_{ab}(0)]/\lambda_{ab}(0)$ for a $36.8°$ [001] tilt symmetric YBCO-GBJ. The solid line shows the dependence expected for a superconductor with a $d_{x^2-y^2}$-symmetry of the order parameter. The measured upturn at low temperatures most likely is due to anomalous Meissner currents.

be explained neither by assuming a pure d-wave nor a pure s-wave symmetry of the order parameter. In both cases $\Delta\lambda_{ab}(T)/\lambda_{ab}(0)$ is expected to monotonously decrease with decreasing temperature. However, as discussed in section 2.3 Andreev bound states can result in an anomalous Meissner current that is flowing in opposite of the usual Meissner current thereby increasing the measured penetration depth. This in turn results in an upturn of the temperature dependence of the London penetration depth at low temperatures. We emphasize, however, that a clear upturn as shown in Fig. 8 has not been observed for all investigated GBJs. At present it is not known what determines the strength of the observed upturn. However, we suppose that interface roughness is an important factor. Additional experiments are required to clarify this issue.

4 Discussion

4.1 Magnetic impurity scenario

Initially, the Anderson-Appelbaum model [16,17] was used by most groups to give an interpretation of the observed zero bias conductance peak in tunneling spectroscopy experiments on HTS [12,30,31,33,34]. However, later on it became clear that the Appelbaum-Anderson model can explain only a few features of the experimental observations. For example, the predicted logarithmic dependence of the conductance on voltage as given by Eq. (1) has been observed for example in Ref. [34]. We note, however, that according to Eq. (1), thermal smearing prevents the observation of a logarithmic dependence for $eV \le k_BT$, i.e. for V smaller than about $1\,\mathrm{mV}$ at a measuring temperature of a few K. Therefore, the logarithmic dependence was verified only for a relatively small voltage/energy scale. Hence, even though the measured data are in fair agreement with the Appelbaum-Anderson prediction, this cannot be considered a definite proof for the validity of this model for the description of the observed zero bias conductance peak.

We now briefly summarize the main arguments against the validity of the Appelbaum-Anderson model. Firstly, a strong argument against the applicability of the Appelbaum-Anderson model is the clear correlation of the temperature for which the zero bias conductance peak disappears and the critical temperature of the investigated HTS that varies between 20 and 90 K. Within the Appelbaum-Anderson model, no such correlation is expected, since the quasiparticle scattering off magnetic impurities leading to the zero bias conductance peak within this model is independent of the onset of superconductivity. In the Appelbaum-Anderson model there is no distinct temperature where the zero bias conductance peak is supposed to disappear. Secondly, the Appelbaum-Anderson model cannot account for the fact that for NCCO a zero bias conductance peak never could be observed. If Cu^{2+}-ions at the grain boundary interface are supposed to act as magnetic impurities causing the zero bias conductance peak, then it is very difficult to explain that the zero bias conductance peak appears only for YBCO, BSCCO, and

LSCO, whereas it is absent for NCCO that contains the same copper-oxygen layers as the basic structural element responsible for superconductivity. We also note that the presence of magnetic scatterers at the grain boundary interface is not related to the presence of a superconducting region with a magnetic impurity concentration n_m [101]. This would include a significant reduction of the critical temperature T_c that is clearly not observed for all of the GBJs.

We next discuss the behaviour in the presence of an applied magnetic field. Provided that there are magnetic impurities at the grain boundary, an applied magnetic field is expected to result in a Zeeman splitting of the impurity levels of $2\delta = 2g\mu_B H$. This has been observed for example in the case of Ta-TaO$_2$-Al junctions [102]. In our GBJ experiments an indirect splitting of the zero bias conductance peak in an applied magnetic field has been observed. Here, indirect means that a splitting could be seen only in the $G(V, H) - G(V, 0)$ curve, i.e. after subtracting the zero field curve. However, firstly at low fields this splitting is much too large than expected according to the Appelbaum-Anderson model and secondly, at larger fields a nonlinear increase of the splitting with increasing applied field is observed. In order to model this behaviour within the Appelbaum-Anderson model a strongly magnetic field dependent g-factor would be required that at low fields is an order of magnitude larger than that observed for metal - metal oxide - metal junctions. For the latter, typically $g \sim 1-3$ independent of the applied magnetic field is obtained. Moreover, in Ref. [13] a finite splitting of the zero bias conductance peak was observed for a SIN-junction already in zero field. Summarizing our discussion we clearly can state that the behaviour of the zero bias conductance peak in the presence of an applied magnetic field cannot be explained within the Appelbaum-Anderson model.

In summary, for all spectroscopic experiments on HTS junctions reporting the observation of zero bias conductance peaks there are strong arguments against the applicability of the Appelbaum-Anderson model [23]. This statement holds for all investigated junction types with at least one HTS electrode, i.e. HTS/I/N-type junctions used in low temperature scanning tunneling spectroscopy, planar HTS/I/N junctions, and HTS/I/HTS type GBJs.

4.2 BTK-model

As discused in section 2.4, for small values of Z the BTK model predicts a peak in the normalized differential conductance at zero voltage that reaches a maximum value of 2. However, this peak should decrease monotonously with increasing voltage and no gap structure is expected to be observed. That is, within the BTK-model the observation of both a gap like structure *and* a zero bias conductance peak is not expected. However, in all the GBJ experiments a clear gap structure and a pronounced zero bias conductance peak always is observed at the same time. Furthermore, in the GBJs no subharmonic gap structures at voltages $2\Delta/n$ were observed that are predicted by the

BTK-model. Finally, the BTK-model does not account for the clear differences between the s-wave material NCCO and the d-wave materials YBCO, BSCCO, and LSCO. This is evident because the BTK-model was developed for conventional BCS superconductors and therefore cannot account for effects related to d-wave superconductivity. It has been pointed out above that the Andreev bound state model represents a generalized BTK-type model that accounts for an arbitrary Z and an anisotropic pair potential. As discussed in the next section this model well describes the experimental data.

4.3 Andreev bound states in d-wave superconductors

In the following we interpret the tunneling experiments on HTS within the Andreev bound state model. We will see that the two essential experimental findings for the HTS-GBJs are naturally explained by this model. Firstly, the clear correlation of the appearance of the zero bias conductance peak in the $G(V)$ curves with the critical temperature is a strong hint that the presence of the zero bias conductance peak is related to the presence of superconductivity. Secondly, the observation that only for d-wave superconductors the zero bias conductance peak is observed gives strong evidence for the correlation of this effect with the symmetry of the order parameter. For NCCO, that is believed to be an s-wave superconductor, and also for conventional low temperature superconductors a zero bias conductance peak could not be observed. This is fully consistent with the Andreev bound state model. In addition, the Andreev bound state model provides a convincing way to explain almost all experimental observations of zero bias conductance peaks in different experimental situations within a *single* model [23].

We first discuss the temperature dependence of the zero bias conductance peak. However, we note that for this dependence so far no complete theoretical description is available at present. In Fig. 9 the normalized conductance at zero bias, $G(0)/G_n$, of a LSCO-GBJ is plotted versus the reduced temperature $t = T/T_c$. For $t > 0.3$, the functional form is close to a $1/T$ dependence. Recently, such dependence has been predicted by Barash *et al.* [42]. However, these authors predict a $1/T$ dependence for small values of t, whereas we find such dependence for large t and, moreover, for a much wider temperature regime (up to $t \sim 1$) than predicted in Ref. [42]. With respect to this discrepancy we note that the faceting and the related angle averaging present in GBJs may have to be taken into account in order to explain the measured temperature dependence of the zero bias conductance peak.

Next we discuss the magnetic field dependence of the zero bias conductance peak. In a recent paper Hu discusses the magnetic field effects that are expected for GBJs including the possibility that the magnetic field might be shielded or screened [23]. However, shielding effects can be definitely ruled out by our experimental results. By studying the magnetic field dependence of the critical current of symmetric HTS-GBJs, we always find a Fraunhofer diffraction pattern like dependencies. From the distance of
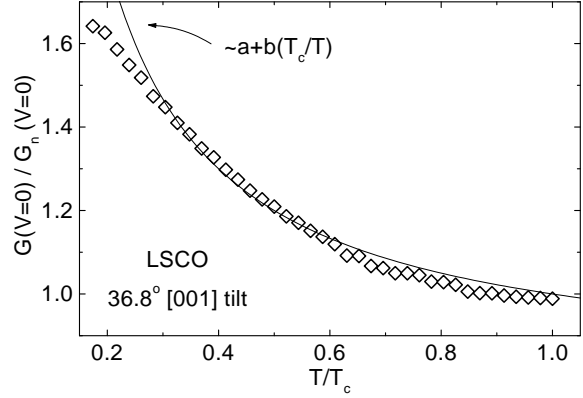

Fig. 9. Normalized conductance at zero bias of a symmetric 36.8^o [001] tilt LSCO-GBJ plotted vs. normalized temperature.

the minima in this dependence we can conclude that the magnetic field penetrates the GBJ as expected. Furthermore, the magnetic field penetrating the grain boundary is enhanced by a factor of order W/d due to flux focusing effects [103]. Here, W is the width of the GBJ and d the thickness of the junction electrodes.

We now discuss the fact that no direct splitting of the zero bias conductance peak in an applied magnetic field is observed in the GBJ experiments, whereas such splitting is expected within the Andreev bound state model. In agreement to our observation no direct splitting of the zero bias conductance peak has been found also by Ekin *et al.* in experiments using planar SIN-type junctions [22]. Furthermore, in experiments using low temperature scanning tunneling spectroscopy a shift or a broadening of the zero bias conductance peak has been observed [33]. Only in some cases a clear split of the zero bias conductance peak in an applied magnetic field including a split at zero applied field was found [13,31]. Hu proposed to explain these different observations with a different behaviour of the magnetic field penetration [23]. However, since the penetration of the magnetic field and flux focusing effects are at least for HTS-GBJs well understood, this cannot be the reason for the absence of a direct splitting of the zero bias conductance peak for GBJs. However, this feature may be understood by considering the faceting of the grain boundary or, equivalently, the interface roughness present in the different junction types. Due to the faceting of the grain boundary barrier the GBJ is known to be formed by a parallel array of many small junctions on a micron and submicron scale with orientations that differ considerably from the nominal misorientation angle of the grain boundary (see Fig. 3). Together with impurity scattering this may lead to a masking of the direct splitting that is expected for junctions with perfectly flat interfaces in an applied field [104].

Although the GBJ experiments show no direct splitting of the zero bias conductance peak in an applied magnetic field, there is a shift of spectral weight from zero to finite energies. This shift of spectral weight results in two peaks in the $G(V,H) - G(V,0)$ curves. Analyzing these

curves we can define a splitting δ as half the peak-to-peak separation. In Fig. 10, the δ values derived in this way are plotted versus H for a LSCO-GBJ at $100\,\text{mK}$ and for a YBCO-GBJ at $4.2\,\text{K}$. Clearly, δ does not vary linearly with the applied field as predicted by the Appelbaum-Anderson model. For all investigated samples δ increases linearly only at small fields below about $2\,\text{T}$. However, for larger fields δ clearly deviates from a linear behaviour and tends to saturate at a constant value at high fields. This is in qualitative agreement with experimental results published very recently [13,31] and theoretical predictions by Fogelström et al. [59]. We note that the splitting δ by definition has to pass through the origin in Fig. 10. That is, from our data we cannot conclude that there is a finite splitting at zero applied magnetic field as observed by Covington et al. [13], although this is suggested by the data shown in Fig. 10. The steep jump from zero to a finite splitting for small applied magnetic field is characteristic for all our samples. Furthermore, the magnetic field dependence of the indirect splitting derived from the $G(V,H) - G(V,0)$ curves of GBJs (see Fig. 10) is consistent with the direct splitting observed by Covington et al. [13] for SIN-type junctions. The reason for this consistency is not obvious and still has to be clarified.
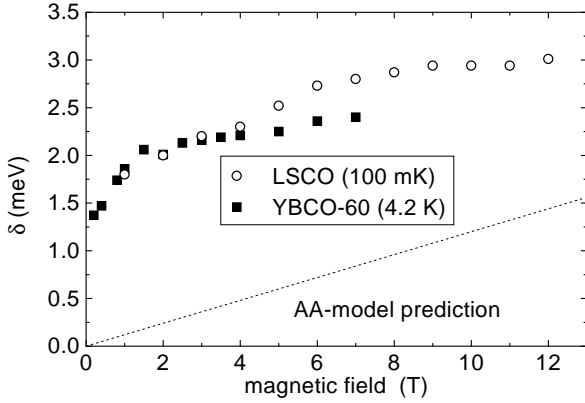

Fig. 10. Splitting δ of the $G(V,H) - G(V,H=0)$ curves of a 36.8^o [001] tilt LSCO-GBJ at $T = 100\,\text{mK}$ and a 24° [001] tilt YBCO-GBJ at $T = 4.2\,\text{K}$ vs. applied magnetic field. Also shown is the Appelbaum-Anderson-model prediction for $g = 2$.

We finally discuss a possible zero field splitting of the zero bias conductance peak. As discussed above, a broken time reversal symmetry state at the surface of a HTS can lead to a split of the zero bias conductance peak in zero magnetic field. Such direct splitting has not been observed in our experiments down to temperatures of $100\,\text{mK}$ for LSCO and down to $4.2\,\text{K}$ for YBCO. Our observations are in agreement to the recent findings of other groups [21,22]. Although the detailed reason for the presence or absence of a zero field splitting of the ZBCO is not clear, one can speculate that the junction property preventing the observation of a direct splitting of the zero bias conductance peak by an applied magnetic field also may result in the absence of any direct splitting in zero applied field. The

most likely reason is the roughness of the surface of the junction electrodes, which in the case of GBJs is caused by the faceting of the grain boundary. Surface roughness together with impurity scattering may lead to a reduction of those quasiparticle trajectories that are responsible for the splitting of the zero bias conductance peak. Furthermore, surface currents along a strongly faceted GBJ could tend to cancel each other. Certainly, this topic has to be clarified in more detail by future theoretical and experimental work. Summarizing our discussion we note that at present it is impossible to make a definitive statement with respect to the occurence of a state with broken time reversal symmetry in HTS-GBJs.

4.4 NCCO-spectra

In the tunneling spectra of NCCO-GBJs never a zero bias conductance peak has been observed. This observation is consistent with an s-wave symmetry of the order parameter in NCCO in contrast to other HTS such as YBCO, BSCCO, or LSCO. Since there is additional experimental evidence that NCCO has a dominant s-wave component of the order parameter, the question arises whether or not NCCO can be viewed as a classical BCS-superconductor. Furthermore, experiments performed on NCCO are highly important in order to clarify the origin of the specific features observed for the d-wave HTS. In this subsection we discuss the tunneling spectra measured for NCCO-GBJs and compare them to those obtained for the d-wave HTS as well as to those expected for classical BCS-superconductors.

Discussing the NCCO spectra shown in Figs. 5 and 7, one might think at first glance that the shape of the spectra resembles that of a typical spectrum of a BCS superconductor, if a finite lifetime of the quasiparticles is taken into account by introducing a smearing parameter Γ according to Dynes et al. [105]. However, looking more closely to the spectra it becomes evident that the measured $G(V)$ curves cannot be described by a BCS type behaviour because of the large conductance at zero bias and the V-shaped gap structure in contrast to the U-shaped structure expected for conventional BCS superconductors. The $G(V)$-curves of NCCO-GBJs resemble by far more those of GBJs fabricated from the other (d-wave) HTS materials. We note that a fit of the measured tunneling spectra using the Dynes formula [105] is possible only in a few cases. Moreover, to obtain a reasonable fit $\Gamma \sim \Delta_0$ has to be used what is difficult to justify. However, the Dynes expression cannot account for both the sharp peaks at the gap edge and the high spectral weight within the gap. Above we argued that NCCO is not a d-wave superconductor because a zero bias conductance peak is completely absent in the tunneling spectra. To account for the observed features an anisotropic s-wave order parameter can be assumed. Then, qualitatively the high spectral weight at zero energy and the absence of the zero bias conductance peak can be explained. We finally note that an extended s-wave symmetry of the order parameter cannot be fully ruled out at present, since the detailed influence

of the surface geometry on the tunneling spectra is not known.

5 Conclusions

Tunneling spectroscopy on differently oriented surfaces of HTS can be used to study the symmetry of the order parameter, since the tunneling spectra are sensitive to the phase of the pair potential. Our comprehensive study of various HTS-GBJs gives clear evidence for the presence of Andreev bound states at the surface of the junction electrodes. For the materials YBCO, BSCCO, and LSCO always a zero bias conductance peak due to Andreev bound states was observed what is consistent with a d-wave symmetry of the order parameter in these materials. In contrast, NCCO never showed a zero bias conductance peak what is consistent with the absence of Andreev bound states and an anisotropic s-wave symmetry of the order parameter. Our results show a clear correlation between the presence of a zero bias conductance peak and superconductivity in the junction electrodes. This gives strong evidence for an explanation of the zero bias conductance peak in terms of Andreev bound states and against an explanation in terms of magnetic impurity scattering. The presence of Andreev bound states at surfaces and interfaces of d-wave HTS also explains the observed anomalous temperature dependence of the London penetration depth. Considering all tunneling data that is available at present from experiments using different tunneling configurations, the vast majority of the measured tunneling spectra can be well explained by taking into account the presence of Andreev bound states at the surface of HTS due to a d-wave symmetry of the order parameter. However, some issues such as the presence of a broken time reversal symmetry state at surfaces of d-wave HTS are still unsettled. In contrast to SIN-junctions, for HTS GBJs no direct splitting of the zero bias conductance peak in zero applied magnetic field was observed.

6 Acknowledgements

References

1. D. J. Van Harlingen, Rev. Mod. Phys. **67**, 515 (1995).
2. D. J. Scalapino, Phys. Rep. **250**, 329 (1995).
3. J. R. Kirtley, C. C. Tsuei, J. Z. Sun, C. C. Chi, Lock See Yu-Jahnes, A. Gupta, M. Rupp, and M. B. Ketchen, Nature **373**, 225 (1995).
4. C. C. Tsuei, J. R. Kirtley, M. Rupp, J. Z. Sun, A. Gupta, M. B. Ketchen, C. A. Wang, Z. F. Ren, J. H. Wang, and M. Bhushan, Science **271**, 329 (1996).
5. L. Buchholtz and G. Zwicknagl, Phys. Rev. **B 23**, 5788 (1981).
6. C. R. Hu, Phys. Rev. Lett. **72**, 1526 (1994); C. Yang and C. R. Hu, Phys. Rev. **B 50**, 16766 (1994).
7. R. Gross, *Grain Boundary Josephson Junctions in the High Temperature Superconductors* in Interfaces in Superconducting Systems, S. L. Shinde and D. Rudman eds, Springer-Verlag, New York (1994), pp. 176-209.
8. R. Gross, L. Alff, A. Beck, O. M. Fröhlich, R. Gerber, R. Gerdemann, A. Marx, B. Mayer, and D. Kölle, Proc. of the *2nd Workshop on HTS Application and New Materials*, D. H. Blank ed, University of Twente, The Netherlands (1995), pp. 8-15.
9. R. Gross, L. Alff, A. Beck, O. M. Fröhlich, D. Kölle, and A. Marx, IEEE Trans. Appl. Supercond. **7**, 2929 (1997).
10. S. Kashiwaya, Y. Tanaka, M. Koyanagi, H. Takashima, and K. Kajimura, Phys. Rev. **B 51**, 1350 (1995).
11. L. Alff, H. Takashima, S. Kashiwaya, N. Terada, H. Ihara, Y. Tanaka, M. Koyanagi, and K. Kajimura, Phys. Rev. **B 55**, R14757 (1997).
12. M. Covington, R. Scheuerer, K. Bloom, and L. H. Greene, Appl. Phys. Lett. **68**, 1717 (1996).
13. M. Covington, M. Aprili, E. Paraoanu, L. H. Greene, F. Xu, J. Zhu, and C. A. Mirkin, Phys. Rev. Lett. **79**, 277 (1997).
14. Yu. S. Barash, A. V. Galaktionov, and A. D. Zaikin, Phys. Rev. **B 52**, 665 (1995).
15. Y. Tanaka and S. Kashiwaya, Phys. Rev. **B 56**, 892 (1997).
16. J. Appelbaum, Phys. Rev. Lett. **17**, 91 (1966); see also Phys. Rev. **154**, 633 (1967).
17. P. W. Anderson, Phys. Rev. Lett. **17**, 95 (1966).
18. Q. Huang, J. F. Zasadzinski, N. Tralshawala, K. E. Gray, D. G. Hinks, J. L. Peng, and R. L. Greene, Nature **347**, 369 (1990).
19. D. H. Wu, J. Mao, J. L. Peng, X. X. Xi, T. Venkatesan, R. L. Greene, and S. M. Anlage, Phys. Rev. Lett. **70**, 85 (1993).
20. A. Andreone, A. Cassinese, A. Di Chiara, R. Vaglio, A. Gupta, and E. Sarnelli, Phys. Rev. **B 49**, 6392 (1994).
21. L. Alff, H. Takashima, S. Kashiwaya, N. Terada, T. Ito, K. Oka, M. Koyanagi, and Y. Tanaka, *Adv. in Supercond. IX*, S. Nakajima and M. Murakami eds, Springer-Verlag, Tokyo (1997), p. 49.
22. J. W. Ekin, Y. Xu, S. Mao, T. Venkatesan, D. W. Face, M. Eddy, and S. A. Wolf, Phys. Rev. **B 56**, 13746 (1997).
23. C. R. Hu, Phys. Rev. **B 57**, 1266 (1998).
24. R. Wilkins, M. Amman, R. E. Soltis, E. Ben-Jacob, and R. C. Jaklevic, Phys. Rev. **B 41**, 8904 (1990).
25. T. Walsh. J. Moreland, R. H. Ono, and T. S. Kalkur, Phys. Rev. Lett. **66**, 516 (1991).
26. L. Y. L. Shen and J. M. Rowell, Phys. Rev. **165**, 633 (1967).
27. E. L. Wolf, *Principles of Electron Tunneling Spectroscopy*, Oxford University Press, New York (1985), p. 356 and p. 395.
28. J. Kondo, Prog. Theor. Phys. **32**, 37 (1964).
29. H. Kroger, L. N. Smith, D. W. Jillie, J. B. Thaxter, R. Aucoin, L. W. Currier, C. N. Potter, D. W. Shaw, and P. H. Willis, IEEE Trans. Magn. **21**, 870 (1985).
30. Thomas Walsh, Int. J. Mod. Phys. **B 6**, 125 (1992).

31. J. Lesueur, L. H. Greene, W. L. Feldmann, and A. Inam, Physica **C 191**, 325 (1992).
32. A. M. Cucolo and R. Di Leo, Phys. Rev. **B 47**, 2916 (1993).
33. S. Kashiwaya, M. Koyanagi, M. Matsuda, and K. Kajimura, Physica **B 194-196**, 2119 (1994).
34. O. M. Fröhlich, P. Richter, A. Beck, R. Gross, and G. Koren, J. Low Temp. Phys. **106**, 243 (1997).
35. J. Zittartz and E. Müller-Hartmann, Z. Phys. **232**, 11 (1969).
36. A. F. Andreev, Zh. Eksp. Teor. Fiz. **46**, 1823 (1964) [Sov. Phys. JETP **19**, 1228 (1964)].
37. D. Rainer, H. Burkhardt, M. Fogelström, and J. A. Sauls, to appear in *Proceedings of SNS'97*, Cape Cod, September 1997; cond-mat/9712234 (1997).
38. M. Atiyah, V. Patodi, and I. Singer, Camb. Phil. Soc. **77**, 43 (1975).
39. Y. Tanaka and S. Kashiwaya, Phys. Rev. Lett. **74**, 3451 (1995).
40. L. J. Buchholtz, M. Palumbo, D. Rainer, and J. A. Sauls, J. Low Temp. Phys. **101**, 1099 (1995).
41. S. Kashiwaya, Y. Tanaka, M. Koyanagi, and K. Kajimura, Phys. Rev. **B 53**, 2667 (1996).
42. Yu. S. Barash, A. A. Svidzinsky, and H. Burkhardt, Phys. Rev. **B 55**, 15282 (1997).
43. M. Koyanagi, S. Kashiwaya, H. Akoh, S. Kohjiro, M. Matsuda, F. Hirayama, and K. Kajimura, Jpn. J. Appl. Phys. **31**, 3525 (1992).
44. Q. Chen and K.-W. Ng, Phys. Rev. **B 45**, 2569 (1992).
45. Ch. Renner and Ø. Fischer, Phys. Rev. **B 51**, 9208 (1995).
46. C. Renner, B. Revaz, J.-Y. Genoud, and Ø. Fischer, J. Low Temp. Phys. **105**, 1083 (1996).
47. C. Renner, B. Revaz, J.-Y. Genoud, K. Kadowaki, and Ø. Fischer, Phys. Rev. Lett. **80**, 149 (1998).
48. Saion Sinha and K.-W. Ng, Phys. Rev. Lett. **80**, 1296 (1998).
49. D. Mandrus, L. Forro, D. Koller, and L. Mihaly, Nature **351**, 460 (1991).
50. I. Iguchi and T. Kusumori, Phys. Rev. **B 46**, 11175 (1992).
51. Th. Becherer, C. Stölzel, G. Adrian, and H. Adrian, Phys. Rev. **B 47**, R14650 (1993).
52. M. Matsumoto and H. Shiba, J. Phys. Soc. Jpn. **64**, 1703 (1995); see also J. Phys. Soc. Jpn. **64**, 3384 (1995).
53. K. Yamada, Y. Nagato, S. Higashitani, and K. Nagai, J. Phys. Soc. Jpn. **65**, 1540 (1996).
54. Y. Tanuma, Y. Tanaka, M. Yamashiro, and S. Kashiwaya, *Adv. in Supercond. IX*, S. Nakajima and M. Murakami eds, Springer-Verlag, Tokyo (1997), p. 307.
55. Y. Tanaka and S. Kashiwaya, Phys. Rev. **B 53**, R11957 (1996).
56. Yu. S. Barash, H. Burkhardt, and D. Rainer, Phys. Rev. Lett. **77**, 4070 (1996).
57. Y. Tanaka and S. Kashiwaya, cond-mat/9803349 (1998).
58. M. Sigrist, D. B. Bailey, and R. B. Laughlin, Phys. Rev. Lett. **74**, 3249 (1995).
59. M. Fogelström, D. Rainer, and J. A. Sauls, Phys. Rev. Lett. **79**, 281 (1997).
60. W. Belzig, C. Bruder, and M. Sigrist, cond-mat/9801107 (1998).
61. F. C. Zhang and T. M. Rice, Phys. Rev. **B 37**, 3759 (1988).
62. Y. Tanuma, Y. Tanaka, M. Ogata, and S. Kashiwaya, to be published in J. Phys. Soc. Jap. **67** (1998); cond-mat/9802243 (1998).
63. K. Kuboki and M. Sigrist, cond-mat/9803032 (1998).
64. S. Kashiwaya, Y. Tanaka, N. Terada, M. Koyanagi, S. Ueno, L. Alff, H. Takashima, Y. Tanuma, and K. Kajimura, to be published in J. Phys. Chem. Solid.
65. H. Won and K. Maki, Phys. Rev. **B 49**, 1397 (1994).
66. W. N. Hardy, D. A. Bonn, D. C. Morgan, R. Liang, and K. Zhang, Phys. Rev. Lett. **70**, 3999 (1993).
67. O. M. Fröhlich, H. Schulze, R. Gross, A. Beck, and L. Alff, Phys. Rev. **B 50**, R13894 (1994).
68. H. Burkhardt, *Thesis*, Universität Bayreuth (1997).
69. H. Walter, W. Prusseit, R. Semerad, H. Kinder, W. Assmann, H. Huber, H. Burkhardt, D. Rainer, and J. A. Sauls, to appear in Phys. Rev. Lett. (1998).
70. G. E. Blonder, M. Tinkham, and T. M. Klapwijk, Phys. Rev. B **25**, 4515 (1982).
71. T. M. Klapwijk, G. E. Blonder, and M. Tinkham, Physica **B 109-110**, 1657 (1982).
72. B. Mayer, L. Alff, T. Träuble, R. Gross, P. Wagner, and H. Adrian, Appl. Phys. Lett. **63**, 996 (1993).
73. A. Marx, U. Fath, W. Ludwig, R. Gross, and T. Amrein, Phys. Rev. **B 51**, 6735 (1995).
74. M. Naito and H. Sato, Appl. Phys. Lett. **67**, 2557 (1995).
75. A. Beck, O. M. Fröhlich, D. Kölle, R. Gross, H. Sato, and M. Naito, Appl. Phys. Lett. **68**, 3341 (1996).
76. H. Sato, M. Naito, and H. Yamamoto, Physica **C 280**, 178 (1997).
77. J. P. Locquet, Y. Jaccard, A. Cretton, E. J. Williams, F. Arrouy, E. Mächler, T. Schneider, Ø. Fischer, and P. Martinoli, Phys. Rev. **B 54**, 7481 (1996).
78. H. Yamamoto, M. Naito, and H. Sato, Phys. Rev. **B 56**, 2852 (1997).
79. K. K. Likharev, *Dynamics of Josephson Junctions and Circuits*, Gordon and Breach, New York (1986).
80. R. Gross and B. Mayer, Physica **C 180**, 235 (1991).
81. R. Gross and B. Mayer, in *Advances in High Temperature Superconductivity*, D. Andreone ed, World Scientific, Singapore (1992), p. 261.
82. J. Halbritter, Phys. Rev. **B 48**, 9735 (1993).
83. O. M. Fröhlich, H. Schulze, A.Beck, B. Mayer, L. Alff, R. Gross, and R. P. Hübener, Appl. Phys. Lett. **66**, 2289 (1995).
84. L. Alff, U. Schoop, R. Gross, R. Gerber, and A. Beck, Physica **C 271**, 339 (1996).
85. O. M. Fröhlich, P. Richter, A.Beck, R. Gross, and G. Koren, J. Low Temp. Phys. **106**, 243 (1997); see also IEEE Trans. Appl. Supercond. **7**, 3189 (1997).
86. A. Marx, L. Alff, and R. Gross, IEEE Trans. Appl. Supercond. **7**, 2719 (1997).
87. S. Kleefisch, L. Alff, U. Schoop, A. Marx, R. Gross, M. Naito, and H. Sato, Appl. Phys. Lett. **72**, 2888 (1998).
88. R. Gross, P. Chaudhari, M. Kawasaki, and A. Gupta, Phys. Rev. **B 42**, 10735 (1990).
89. B. Kabius, J. W. Seo, T. Amrein, U. Dähne, A. Scholen, M. Siegel, K. Urban, and L. Schultz, Physica **C 231**, 123 (1994).
90. J. Mannhart, H. Hilgenkamp, B. Mayer, Ch. Gerber, J. R. Kirtley, K. A. Moler, and M. Sigrist, Phys. Rev. Lett. **77**, 2782 (1996).
91. H. Hilgenkamp, J. Mannhart, and B. Mayer, Phys. Rev. **B 53**, 14586 (1996).
92. L. Alff, A. Beck, R. Gross, A. Marx, S. Kleefisch, Th. Bauch, H. Sato, M. Naito, and G. Koren, accepted by Phys. Rev. **B**; cond-mat/9805162 (1998).

93. H. Ding, T. Yokoya, J. C. Campuzano, T. Takahashi, M. Randeria, M. R. Norman, T. Mochiku, K. Kadowaki, and J. Giapintzakis, Nature **382**, 51 (1996).
94. A. G. Loeser, Z.-X. Shen, D. S. Dessau, D. S. Marshall, C. H. Park, P. Fournier, and A. Kapitulnik, Science **273**, 325 (1996).
95. N. Miyakawa, P. Guptasarma, J. F. Zasadzinski, D. G. Hinks, and K. E. Gray, Phys. Rev. Lett. **80**, 157 (1998).
96. In the following we will refer to the hole doped superconductors as d-wave superconductors. We note that for example LSCO is sometimes considered as s-wave symmetry type superconductor at low temperatures: N. S. Achsaf, D. Goldschmidt, and G. Deutscher, J. Low Temp. Phys. **105**, 329 (1996).
97. M. B. Walker and P. Pairor, cond-mat/9803079 (1998).
98. L. Alff, H. Takashima, S. Kashiwaya, N. Terada, T. Ito, K. Oka, Y. Tanaka, and M. Koyanagi, Physica **C 282-287**, 1485 (1997).
99. M. Nantoh, M. Kawasaki, T. Hasegawa, K. Fujito, W. Yamaguchi, H. Koinuma, and K. Kitazawa, Physica **C 242**, 277 (1995).
100. M. Zittartz, *Diploma Thesis*, Universität zu Köln (1997).
101. Yu. N. Ovchinnikov and V. Z. Kresin, Phys. Rev. **B 54**, 1251 (1996).
102. J. A. Appelbaum and L. Y. L. Shen, Phys. Rev. **B 5**, 544 (1972).
103. P. A. Rosenthal, M. R. Beasley, K. Char, M. S. Colclough, and G. Zaharchuk, Appl. Phys. Lett. **59**, 3482 (1991).
104. M. Fogelström and J. Sauls, private communication.
105. R. C. Dynes, V. Narayanamurti, and J .P. Garno, Phys. Rev. Lett. **41**, 1509 (1978).